Available online at www.sciencedirect.com
ScienceDirect
Journal of the European Ceramic Society 31 (2011) 2975–2980
www.elsevier.com/locate/jeurceramsoc

Effects of $Bi_2Mo_2O_9$ addition on the sintering characteristics and microwave dielectric properties of $BiSbO_4$ ceramics

Sea-Fue Wang *, Yung-Fu Hsu, Yuh-Ruey Wang, Yong-Han Huang

Department of Materials and Mineral Resources Engineering, National Taipei University of Technology, 1, Sec. 3, Chung-Hsiao E. Rd., Taipei 106, Taiwan, ROC

Received 22 February 2011; received in revised form 24 June 2011; accepted 4 July 2011
Available online 4 August 2011

Abstract

In this study, densification, microstructural evolution and microwave dielectric properties of $(1-x)BiSbO_4$–$xBi_2Mo_2O_9$ ceramics ($x = 0$–0.25) were investigated. $Bi_2Mo_2O_9$ was selected as the sintering aid as well as the modifier of the dielectric properties for $BiSbO_4$ ceramic. In comparison with pure $BiSbO_4$ densified at 1100 °C, the $0.75BiSbO_4$–$0.25Bi_2Mo_2O_9$ composites emerged to reach maximum sintering density at 775 °C. No other second phase was detected while the microstructure exhibited a bimodal grain size distribution as both 1–2 μm large grains of $Bi_2Mo_2O_9$ and 0.2–0.5 μm fine grains of $BiSbO_4$ were observed. The ceramic with the best performance in terms of microwave dielectric properties in this system is found to be the $0.82BiSbO_4$–$0.18Bi_2Mo_2O_9$ composite, which reports a ε_r of 24.3, a $Q \times f$ of 24,019 GHz, and a τ_f of −4 ppm/°C when sintered at 825 °C.

Keywords: Dielectric properties; Sintering; Composites; Grain size; $BiSbO_4$

1. Introduction

A high dielectric constant, high dielectric loss quality ($Q > 2000$), and near zero temperature coefficient of resonant frequency τ_f are required for applications in microwave devices, such as cellular phones, global positioning systems and personal communication systems. A high dielectric constant makes it possible to reduce the size of the material by a factor of $1/\varepsilon_r^{1/2}$ to facilitate considerable reduction in circuit size. A high Q value, on the other hand, enables low insertion loss and low bandwidth of the resonance frequency, both essential for achieving high frequency selectivity and stability in microwave transmitter components. A near-zero τ_f is further required for stabilizing frequency against temperature.

The sintering temperatures of common microwave dielectric ceramics fall in the range of 1200–1500 °C. The sintering temperatures of $Ba_2Ti_9O_{20}$, $Ba_{6-x}Ln_{8+2x/3}Ti_{18}O_{54}$, and $(Zr,Sn)TiO_4$ systems, for instance, are respectively 1300 °C, 1350 °C and 1400 °C,[1–3] all much higher than the melting temperature of Ag (961 °C) or Cu (1064 °C). Several methods have been developed in response to the growing interest in new materials with a low sintering temperature. One method involves the investigation of glass-forming additives on the properties of established microwave materials.[4] Another way is the use of new material systems with a lower sintering temperature.[5,6] Recently, researchers have shown that bismuth-based ceramics, including the binary systems of Bi_2O_3–$(Nb,Ta)_2O_5$ and Bi_2O_3–$(Sb,Ta)_2O_5$,[7–9] the ternary systems of Bi_2O_3–CaO–Nb_2O_5 and Bi_2O_3–ZnO–$(Nb,Ta)_2O_5$,[7,10,11] possess low sintering temperatures ranging from 900 to 1100 °C and excellent microwave dielectric characteristics.

Examining the microwave dielectric properties of $BiSbO_4$ ceramic, the study of Wang and colleagues[12] reported a dielectric constant (ε_r) of 19, a $Q \times f$ value of 70,000 GHz, and a temperature coefficient of resonant frequency (τ_f) of −62 ppm/°C at a sintering temperature of 1080 °C. Additives of the V_2O_5–CuO and B_2O_3–CuO systems were added to further lower the sintering temperature of $BiSbO_4$ ceramic.[13,14] $BiSbO_4$ ceramic sintered with 1 wt% of V_2O_5–CuO and 0.6 wt% of B_2O_3–CuO at 930 °C demonstrated respectively the following microwave dielectric properties: $\varepsilon_r \approx 19$, $Q \times f \approx 40{,}000$ GHz, and $\tau_f \approx -71.5$ ppm/°C, and $\varepsilon_r \approx 19.47$, $Q \times f \approx 45{,}405$ GHz, and $\tau_f \approx -66.2$ ppm/°C.

* Corresponding author. Tel.: +886 2 2771 2171x2735; fax: +886 2 2731 7185.
E-mail addresses: sfwang@ntut.edu.tw, seafuewang@yahoo.com (S.-F. Wang).

0955-2219/$ – see front matter © 2011 Elsevier Ltd. All rights reserved.
doi:10.1016/j.jeurceramsoc.2011.07.005

Instead of adding sintering additives, the study explores the different approach of introducing the low-sintering-temperature microwave dielectric ceramic $Bi_2Mo_2O_9$ not only to lower the sintering temperature but also to improve the microwave dielectric properties of $BiSbO_4$ ceramic. It was recently reported that $Bi_2Mo_2O_9$ ceramic could be sintered at 620 °C while still sustaining good microwave dielectric properties of $\varepsilon_r \approx 38$, $Q \times f \approx 12{,}500$ GHz, and $\tau_f \approx \pm 31$ ppm/°C.[15] The effects of $Bi_2Mo_2O_9$ addition on the sintering characteristics and microwave dielectric properties of $BiSbO_4$ are discussed based on the results of X-ray diffraction (XRD), scanning electron microscopy (SEM), thermal analysis, and dielectric characterization.

2. Experimental procedure

$BiSbO_4$ and $Bi_2Mo_2O_9$ in various ratios (ranging from 0 m% to 25 m%) were prepared using the solid-state reaction technique. Highly pure (>99.9% purity) Bi_2O_3 (Acros, Reagent grade), Sb_2O_3 (STREM, Reagent grade), and Mo_2O_3 (Alfa, Reagent grade) were used as raw materials. Oxides based on the constituents calculated from the ratio of $BiSbO_4$ and $Bi_2Mo_2O_9$ were mixed and milled in methyl alcohol solution using polyethylene jars and zirconia balls for 24 h and then oven-dried at 80 °C for overnight. After drying, the powders were calcined at 850 °C for 4 h at a heating rate of 5 °C/min, and then re-milled in methyl alcohol for 24 h. The powders were added with 5 wt% of 15%-PVA solution and pressed into disc-shaped compacts under a uniaxial pressure of 140 MPa. The samples were then heat treated at 550 °C for 4 h to eliminate PVA, followed by sintering at 700–1200 °C for 2 h (heating rate = 5 °C/min), depending on the ceramic composition. Bulk densities of the sintered samples were measured using the Archimedes method with de-ionized water. Phase identification of the calcined powders as well as the sintered bulk ceramics was performed using X-ray diffraction (XRD, Simens D5000). Differential thermal and thermogravimetric analyses (DTA/TGA) were then conducted in a Pt crucible at a heating rate of 10 °C/min, using a Perkin-Elmer calorimeter (Series 1700 DTA), on the mixtures to evaluate the melting reactions. The samples used for SEM observation were thermally etched, and the microstructures were observed by scanning electron microscopy (SEM, JEOL 6500F) with an energy-dispersive spectroscopy (EDS). The densified cylindrical samples were polished to achieve an exact thickness of 5 mm for measuring microwave properties. The dielectric constants and unloaded Q values at microwave frequencies were measured in the $TE_{01\delta}$ mode using the Hakki and Colleman method[16] and a network analyzer (HP 8722ES). Measurements of the temperature coefficient of the resonant frequency τ_f in the temperature range of 25–85 °C were performed in a Delta Design box furnace. The τ_f was defined by $(f_T - f_{25})/(f_{25}(T - 25\,°C))$.

3. Results and discussion

Fig. 1 shows the apparent densities of the $(1-x)BiSbO_4$–$xBi_2Mo_2O_9$ composite ceramics sintered

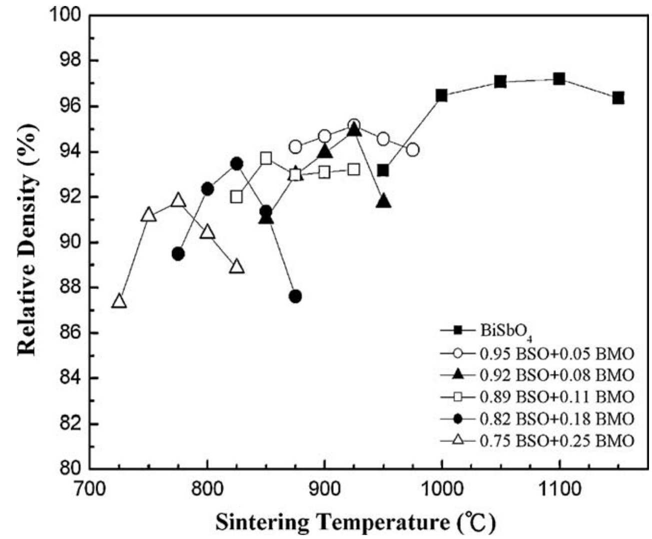

Fig. 1. Sintered densities of $(1-x)BiSbO_4$–$xBi_2Mo_2O_9$ composite ceramics sintered at different temperatures for 2 h.

at different temperatures. Pure $BiSbO_4$ reached maximum densification at 1100 °C in 2 h, and a sintered density exceeding 95% theoretical density (8.459 g/cm^3)[17] was achieved. Addition of $Bi_2Mo_2O_9$ triggered a significant drop in the densification temperature. The $(1-x)BiSbO_4$–$xBi_2Mo_2O_9$ composite ceramics with $x = 0.05$ reached maximum densification at

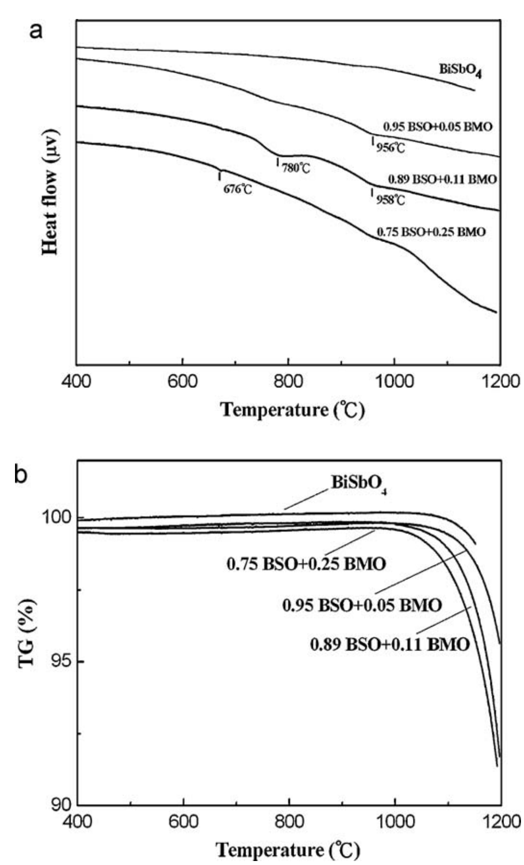

Fig. 2. DTA/TGA curves of $(1-x)BiSbO_4$–$xBi_2Mo_2O_9$ composite ceramics sintered at different temperatures.

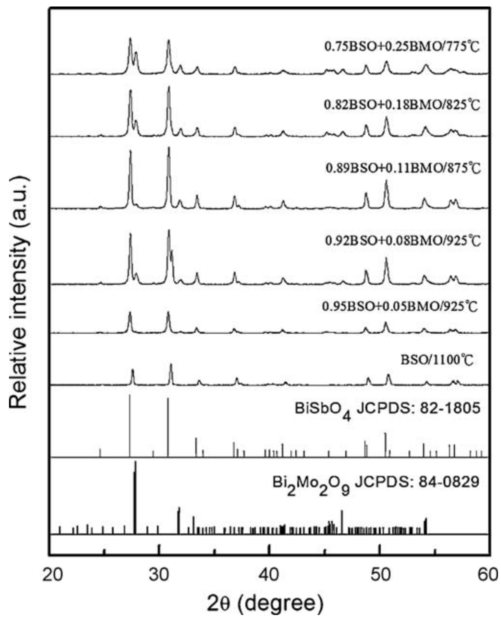

Fig. 3. XRD patterns of $(1-x)BiSbO_4$–$xBi_2Mo_2O_9$ composite ceramics sintered at different temperatures.

925 °C. As the x approached 0.25, maximum densification was achieved at 775 °C. The maximum theoretical density of the ceramics decreased with increasing $Bi_2Mo_2O_9$ content, ranging from 92% to 98%. It should be noted that no precalcination of $BiSbO_4$ and $Bi_2Mo_2O_9$ was performed before mixing the composite. The $BiSbO_4$–$Bi_2Mo_2O_9$ composites were prepared directly using the metal oxides. Proportional ratios of Bi_2O_3, Sb_2O_3, and Mo_2O_3 were mixed, calcined at 850 °C, re-milled, pelletized and then sintered. The study found that precalcination of the $BiSbO_4$ and $Bi_2Mo_2O_9$ compounds led to warped dimension after sintering. Common low-fire microwave ceramics often encounter a narrow processing window due to high vapor pressure at high temperatures, causing inhomogeneous composition and microstructural evolution and resulting in the inability to reproduce the microwave dielectric properties. It is worth noting that the sintered $(1-x)BiSbO_4$–$xBi_2Mo_2O_9$ ceramics appeared to have a homogeneous sintering shrinkage and a uniform color indicating homogeneity of the composition. There was no visible weight loss due to evaporation of various species during sintering.

It was found from the XRD and DTA/TGA results that the formation of $Bi_2Mo_2O_9$ and $BiSbO_4$ phases in the mixture of Bi_2O_3, Sb_2O_3, and Mo_2O_3 during calcination process was proceeded at the temperatures around 428 °C and 792 °C, fairly close to those reported in the literature.[12,15] Fig. 2 shows the DTA/TGA curves of the calcined $(1-x)BiSbO_4$–$xBi_2Mo_2O_9$ powders heated up to 1200 °C. For pure $BiSbO_4$, as indicated by Fig. 2(a), there is no reaction below the temperatures measured since the endothermic melting reaction occurred at the temperature of ≈1276 °C.[20] Three small endothermic peaks emerged respectively at 676, 780 and 958 °C for the $BiSbO_4$ powders with various amounts of $Bi_2Mo_2O_9$, with the former two corresponding to the incongruent melting points of $Bi_2Mo_2O_9$[18] and the last one to the irreversible phase transition temperature of $BiSbO_4$. Fig. 2(b) presents the TGA results of the $BiSbO_4$ powders with various amounts of $Bi_2Mo_2O_9$. Significant weight loss was observed at temperatures higher than ≈1100 °C for pure $BiSbO_4$ and ≈1000 °C for $0.75BiSbO_4$–$0.25Bi_2Mo_2O_9$.

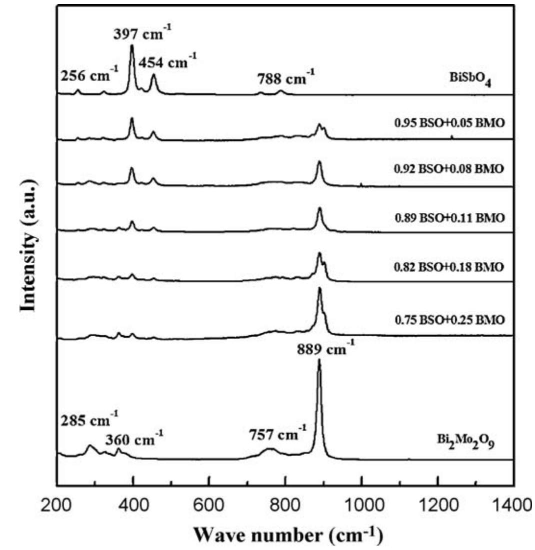

Fig. 4. Raman spectra of $(1-x)BiSbO_4$–$xBi_2Mo_2O_9$ composite ceramics sintered at different temperatures.

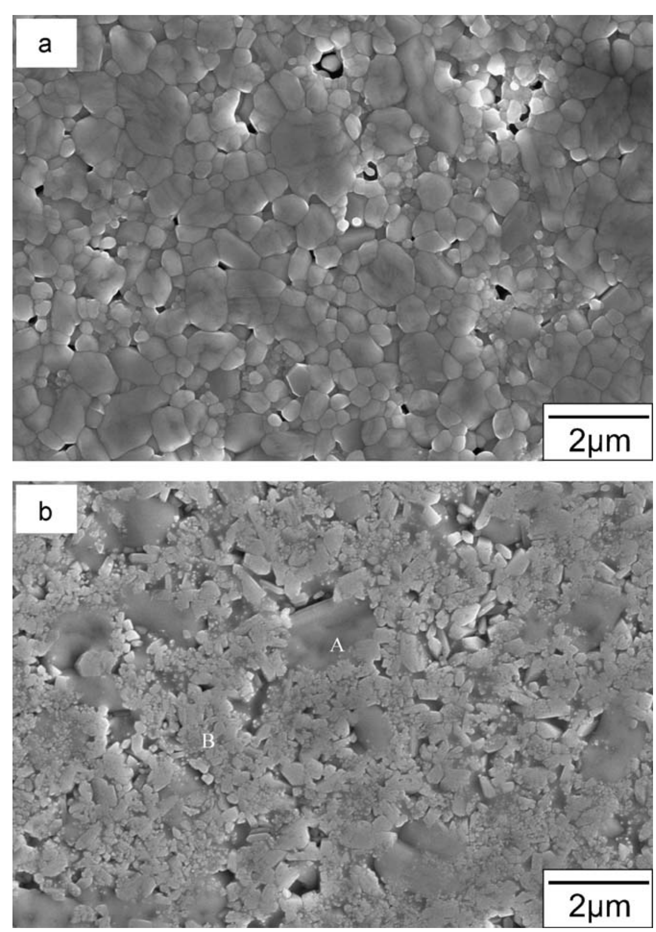

Fig. 5. SEM micrographs of (a) $BiSbO_4$ ceramic sintered at 1100 °C for 2 h, and (b) $0.75BiSbO_4$–$0.25Bi_2Mo_2O_9$ composites sintered at 775 °C for 2 h.

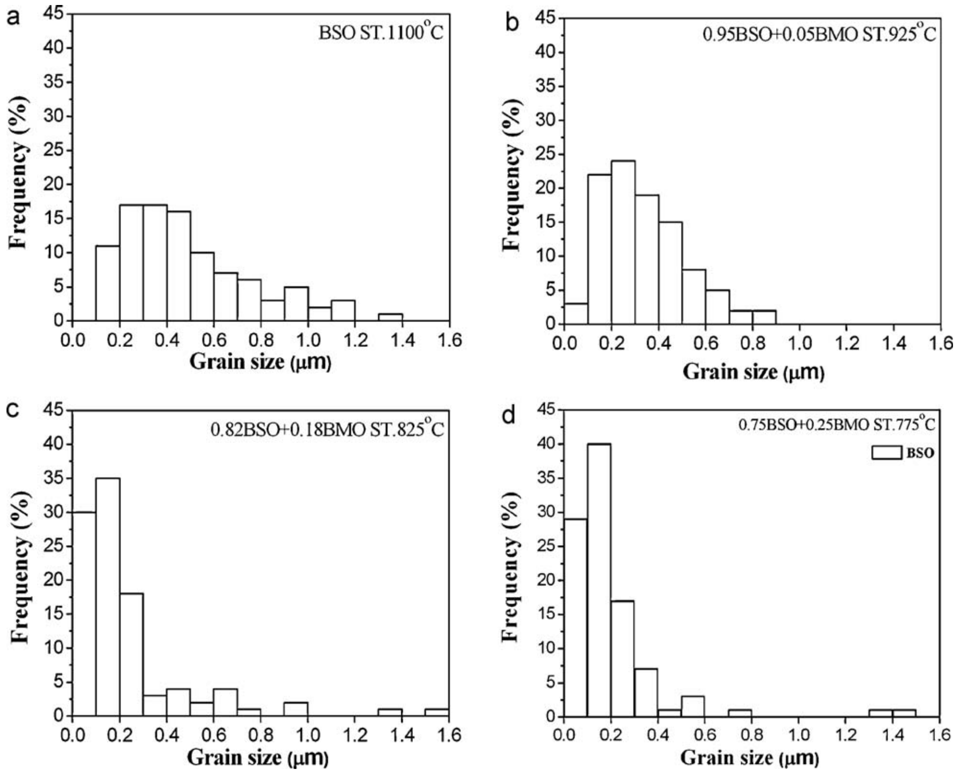

Fig. 6. Grain size distributions of the $BiSbO_4$ matrix for (a) $BiSbO_4$ ceramic sintered at 1100 °C, (b) $0.95BiSbO_4$–$0.05Bi_2Mo_2O_9$ ceramic sintered at 925 °C, (c) $0.82BiSbO_4$–$0.18Bi_2Mo_2O_9$ ceramic sintered at 825 °C, and (d) $0.75BiSbO_4$–$0.25Bi_2Mo_2O_9$ ceramic sintered at 775 °C.

A comparison of the data in Figs. 1 and 2(b) suggests that addition of $Bi_2Mo_2O_9$ not only reduces the sintering temperature of the $BiSbO_4$ ceramic but also pushes the maximum densification temperature away from the onset temperatures of the rapid weight loss due to evaporation.

Fig. 3 illustrates the XRD patterns of the $(1-x)BiSbO_4$–$xBi_2Mo_2O_9$ ceramics with various $Bi_2Mo_2O_9$ contents. The XRD patterns were identified as $BiSbO_4$ and $Bi_2Mo_2O_9$ phases. $BiSbO_4$ has a monoclinic structure [I2/c space group, $a = 5.4690$, $b = 4.8847$, $c = 11.8252$ Å, and $\beta = 101.131°$].[19] X-ray diffraction data show that $Bi_2Mo_2O_9$ has a monoclinic structure (P21/n), with lattice parameters $a = 11.9664$, $b = 10.8089$, $c = 11.8871$ Å, and $\beta = 90.13°$.[15] The intensities of the peaks corresponding to the $BiSbO_4$ and $Bi_2Mo_2O_9$ phases are consistent with their contents in the starting powders. No other second phase has been found in the XRD results, except the $BiSbO_4$ and $Bi_2Mo_2O_9$ phases. Fig. 4 shows the Raman spectra (wavelength of excitation 514 nm) of the $(1-x)BiSbO_4$–$xBi_2Mo_2O_9$ composite ceramics sintered at different temperatures. The Raman spectra located at 397, 454, 788, and 256 cm^{-1} corresponded to $BiSbO_4$ while the ones at 889, 757, 360, and 285 cm^{-1} corresponded to $Bi_2Mo_2O_9$. Consistent with the XRD results shown in Fig. 3, the characteristic peaks of $Bi_2Mo_2O_9$ rose and that of $BiSbO_4$ declined with increased $Bi_2Mo_2O_9$ addition.

Typical SEM micrographs for the $(1-x)BiSbO_4$–$xBi_2Mo_2O_9$ ceramics, as shown in Fig. 5(a) and (b), corresponded respectively to the $BiSbO_4$ ceramic sintered at 1100 °C and the $0.75BiSbO_4$–$0.25Bi_2Mo_2O_9$ composite sintered at 775 °C. The pure $BiSbO_4$ ceramic shows a microstructure composed of angular grains in the sizes of 0.2–1 μm. With the addition of $Bi_2Mo_2O_9$ in the $BiSbO_4$ ceramic, the microstructure exhibited a bimodal grain size distribution as both 1–2 μm large grains and 0.2–0.5 μm fine grains were observed. EDS results confirmed that the large grains of area A and the fine grains of area B corresponded respectively to the $Bi_2Mo_2O_9$ and $BiSbO_4$ ceramics, all in agreement with the XRD and Raman results presented in Figs. 3 and 4. The $Bi_2Mo_2O_9$ addition reduced the sintering temperature of $BiSbO_4$ and thus inhibited the grain growth of $BiSbO_4$ matrix. The SEM microstructures also show no second phase along the grain boundaries, thus confirming the XRD results in Fig. 3. As indicated by Fig. 6 that shows the grain size distributions of the $BiSbO_4$ matrix for the $BiSbO_4$ ceramic (sintered at 1100 °C), the $0.95BiSbO_4$–$0.05Bi_2Mo_2O_9$ ceramic (sintered at 925 °C), the $0.82BiSbO_4$–$0.18Bi_2Mo_2O_9$ ceramic (sintered at 825 °C), and the $0.75BiSbO_4$–$0.25Bi_2Mo_2O_9$ ceramic (at 775 °C), it is evident that the grain size distribution of the $BiSbO_4$ matrix became narrower and shifted to the smaller grain size as the $Bi_2Mo_2O_9$ content increased. The average grain size of the $BiSbO_4$ matrix decreased from 0.45 to 0.12 μm as the $Bi_2Mo_2O_9$ content escalated from 0 to 25 m%. On the other hand, the grain size of the $Bi_2Mo_2O_9$ phase ranged from 0.5 to 2.5 μm, showing no obvious variance along with its content in the composites. The shrinkage in the grain size of the $BiSbO_4$ matrix is mainly due to the significant reduction in the sintering temperature of the composites with the growth in the $Bi_2Mo_2O_9$ content.

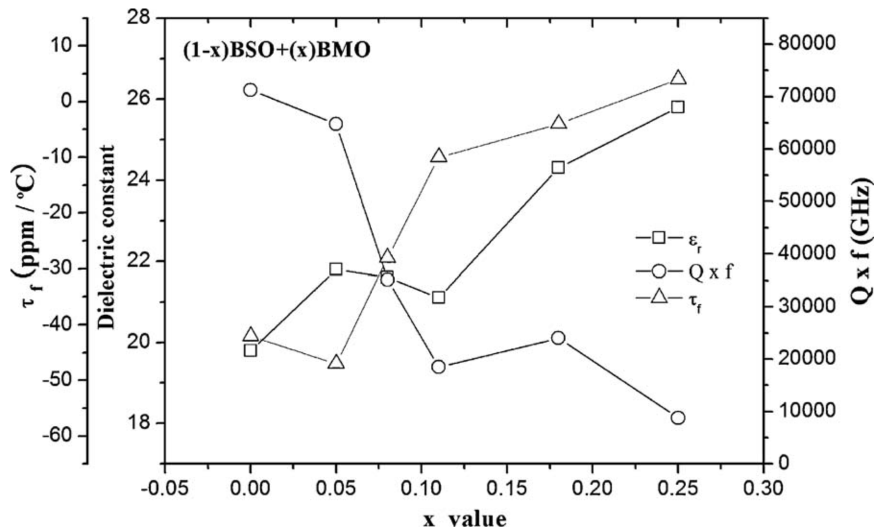

Fig. 7. Dielectric constant, quality factors, and temperature coefficients of $(1-x)BiSbO_4$–$xBi_2Mo_2O_9$ composite ceramics with various x values.

Table 1
Microwave dielectric properties of $BiSbO_4$–$Bi_2Mo_2O_9$ composite ceramics with various x values.

Composition	ε_r	$Q \times f$ (GHz)	τ_f (ppm/°C)
$BiSbO_4$	19.8	71,291	−42
$0.95BiSbO_4$–$0.05Bi_2Mo_2O_9$	21.8	64,780	−47
$0.92BiSbO_4$–$0.08Bi_2Mo_2O_9$	21.6	35,115	−28
$0.89BiSbO_4$–$0.11Bi_2Mo_2O_9$	21.1	18,470	−10
$0.82BiSbO_4$–$0.18Bi_2Mo_2O_9$	24.3	24,019	−4
$0.75BiSbO_4$–$0.25Bi_2Mo_2O_9$	25.8	8,735	+4

The microwave dielectric properties, including dielectric constant (ε_r), quality factor ($Q \times f$), and temperature coefficient of resonant frequency (τ_f), of the $(1-x)BiSbO_4$–$xBi_2Mo_2O_9$ ceramics with maximum densification are shown in Fig. 7 and summarized in Table 1. The dielectric constants of the $(1-x)BiSbO_4$–$xBi_2Mo_2O_9$ ceramics ranged from 19.8 to 25.8. The ceramic with $x=0$ ($BiSbO_4$) reported the lowest dielectric constant of 19.8, as shown in Fig. 7. The dielectric constant of the $(1-x)BiSbO_4$–$xBi_2Mo_2O_9$ ceramics increased with the growth in $Bi_2Mo_2O_9$ content, since the $Bi_2Mo_2O_9$ registers a dielectric constant of 38.[15] The $Q \times f$ values of the $(1-x)BiSbO_4$–$xBi_2Mo_2O_9$ ceramics experienced a drastic decline with increased $Bi_2Mo_2O_9$ substitution, for example, from 71,291 for pure $BiSbO_4$ ceramics to 8735 for its $0.75BiSbO_4$–$0.25Bi_2Mo_2O_9$ counterpart. The τ_f value varied from −42 to +4 ppm/°C and grew less negative as the added amount of $Bi_2Mo_2O_9$ rose. The $0.82BiSbO_4$–$0.18Bi_2Mo_2O_9$ ceramics emerged to be the ceramic with the best performance in terms of microwave dielectric properties (a ε_r of 24.3, a $Q \times f$ of 24,019 GHz, and a τ_f of −4 ppm/°C) when sintered at 825 °C.

4. Conclusion

Based on the study results, the densification, thermal properties, microstructural evolution and dielectric properties of the $(1-x)BiSbO_4$–$xBi_2Mo_2O_9$ composites ($x=0$–0.25) are summarized as follows.

1. $BiSbO_4$ reaches maximum densification at 1000 °C, and the $0.75BiSbO_4$–$0.25Bi_2Mo_2O_9$ composites achieve maximum sintering density at 775 °C.
2. In the XRD patterns and Raman spectra of the composites, $BiSbO_4$ and $Bi_2Mo_2O_9$ phases are identified while no other second phase has been found. With addition of $Bi_2Mo_2O_9$ in the $BiSbO_4$ ceramic, the microstructure exhibits a bimodal grain size distribution indicated by the presence of both 1–2 μm large grains and 0.2–0.5 μm fine grains.
3. The microwave dielectric properties of the pure $BiSbO_4$ sintered at 1100 °C can be summarized as $\varepsilon_r \approx 19.8$, $Q \times f \approx 71{,}291$ GHz, and $\tau_f \approx -42$ ppm/°C. The ceramic with the best performance in terms of microwave dielectric properties in this system goes to the $0.82BiSbO_4$–$0.18Bi_2Mo_2O_9$ ceramic, which reports a ε_r of 24.3, a $Q \times f$ of 24,019 GHz, and a τ_f of −4 ppm/°C when sintered at 825 °C.

References

1. Wang SF, Chung CC, Chu JP. Effects of additives on the microstructure and dielectric properties of $Ba_2Ti_9O_{20}$ microwave ceramic. *J Mater Res* 2003;**18**:1179–87.
2. Xu Y, He Y. Polymeric precursor synthesis of $Ba_{6-3x}Sm_{8+2x}Ti_{18}O_{54}$ ceramic powder. *Ceram Int* 2002;**28**:75–8.
3. Wolfram G, Gobel HE. Existence range, structural and dielectric properties of $Zr_xTi_ySn_zO_4$ ceramics ($x+y+z=2$). *Mater Res Bull* 1952;**16**:1455–63.
4. Takada T, Wang SF, Yoshikawa S, Jang SJ, Newnham RE. Effects of glass additions on BaO–TiO_2–WO_3 for microwave ceramics. *J Am Ceram Soc* 1994;**77**:1909–16.
5. Borisevich A, Davies PK. Microwave dielectric properties of $Li_{1+x-y}M_{1-x-3y}Ti_{x+4y}O_3$ ($M=Nb^{5+}$, Ta^{5+}) solid solutions. *J Eur Ceram Soc* 2001;**21**:1719–22.
6. Turky G, Dawy M. Spectral and electrical properties of ternary (TeO_2–V_2O_5–Sm_2O_3) glasses. *Mater Chem Phys* 2002;**77**:48–59.
7. Kagata H, Inoue T, Kato J, Kameyama I. Low-fire bismuth-based dielectric ceramics for microwave use. *Jpn J Appl Phys* 1992;**31**:3152–5.

8. Zhou D, Wang H, Yao X, Pang LX. Sintering behavior phase evolution, and microwave dielectric properties of $Bi(Sb_{1-x}Ta_x)O_4$ ceramics. *J Am Ceram Soc* 2008;**91**:2228–31.
9. Valant M, Suvorov D. Dielectric properties of the fluorite-like Bi_2O_3–Nb_2O_5 solid solution and the tetragonal Bi_3NbO_7. *J Am Ceram Soc* 2003;**86**:939–44.
10. Shen B, Dong YM, Zhai JW. Microwave dielectric properties of $Bi_2(Zn_{1/3}Ta_{2/3})_2O_7$–$CaTiO_3$ composite ceramics. *J Ferroelectr* 2007;**356**:140–5.
11. Valant M, Davies PK. Crystal chemistry and dielectric properties of chemically substituted $(Bi_{1.5}Zn_{1.0}Nb_{1.5})O_7$ and $Bi_2(Zn_{2/3}Nb_{4/3})O_7$ pyrochlores. *J Am Ceram Soc* 2000;**83**:147–53.
12. Zhou D, Wang H, Yao X, Pang LX. Dielectric behavior and cofiring with silver of monoclinic $BiSbO_4$ ceramic. *J Am Ceram Soc* 2008;**91**:1380–3.
13. Zhou D, Wang H, Pang LX, Yao X. Low-firing of $BiSbO_4$ microwave dielectric ceramic with V_2O_5–CuO addition. *Mater Chem Phys* 2010;**11**:149–52.
14. Zhou D, Wang H, Pang LX, Yao X, Wu XG. Low temperature firing of $BiSbO_4$ microwave dielectric ceramic with B_2O_3–CuO addition. *Mater Chem Phys* 2010;**119**:149–52.
15. Zhou D, Wang H, Yao X, Pang LX. Microwave dielectric properties of low temperature firing $Bi_2Mo_2O_9$ ceramic. *J Am Ceram Soc* 2008;**91**:3419–22.
16. Bart JCJ, Petrini G, Glordano N. The binary oxide system TeO_2–MoO_3. *Z Anorg Allg Chem* 1975;**412**:258–70.
17. Kennedy B. X-ray powder diffraction study of $BiSbO_4$. *Powder Diffr* 1994:9164–7.
18. Zhou D, Wang H, Pang LX, Randall CA, Yao X. Bi_2O_3–MoO_3 binary system: an alternative ultralow sintering temperature microwave dielectric. *J Am Ceram Soc* 2009;**92**:2242–6.
19. Valant M, Suvorov D. Processing and dielectric properties of sillenite compounds $Bi_{12}MO_{20-\delta}$ (M = Si, Ge, Ti, Pb, Mn, $B_{1/2}P_{1/2}$). *J Am Ceram Soc* 2001;**12**:2900–4.
20. Liang JK, Zhang YL, Fang X. *Diwen Wuli Xuebao* 1992;**14**:161–6.